A Two-stage Stochastic Mixed-integer Programming Model for Resilience Enhancement of Active Distribution Networks

Hongzhou Chen, Jian Wang, *Member*, *IEEE*, Jizhong Zhu, *Fellow*, *IEEE*, Xiaofu Xiong, *Member*, *IEEE*, Wei Wang, *Member*, *IEEE*, and Hongrui Yang

***Abstract*—Most existing distribution networks are difficult to withstand the impact of meteorological disasters. With the development of active distribution networks (ADNs), more and more upgrading and updating resources are applied to enhance the resilience of ADNs. A two-stage stochastic mixed-integer programming (SMIP) model is proposed in this paper to minimize the upgrading and operation cost of ADNs by considering random scenarios referring to different operation scenarios of ADNs caused by disastrous weather events. In the first stage, the planning decision is formulated according to the measures of hardening existing distribution lines, upgrading automatic switches, and deploying energy storage resources. The second stage is to evaluate the operation cost of ADNs by considering the cost of load shedding due to disastrous weather and optimal deployment of energy storage systems (ESSs) under normal weather condition. A novel modeling method is proposed to address the uncertainty of the operation state of distribution lines according to the canonical representation of logical constraints. The progressive hedging algorithm (PHA) is adopted to solve the SMIP model. The IEEE 33-node test system is employed to verify the feasibility and effectiveness of the proposed method. The results show that the proposed model can enhance the resilience of the ADN while ensuring economy.**

***Index Terms*—Active distribution network (ADN), resilience, disastrous weather event, stochastic programming.**

NOMENCLATURE

A. Indices

(i,j)	Line index
i,j,k	Node indexes
R	Resilience level of active distribution networks (ADNs)
R_0	Resilience level of ADNs in resilient state
R_{pe}	Resilience level of ADNs in post-event degraded state
s	Scenario index
t	Time index

B. Sets and Matrices

μ_i	Mean of points in ψ_i
ψ_i	Set of unsupplied load vectors
φ_i	Scenario of ψ_i
$\boldsymbol{c}^{\mathrm{T}}$	Cost coefficient vector
$\boldsymbol{f}_s^{\mathrm{T}}$	Associated cost coefficient vector
L	Set of lines
N	Set of nodes
$\mathcal{Q}_s$	Set of problem constraints
S	Set of scenarios
SW	Set of lines with switches
T	Set of time spans
$\boldsymbol{x}$	Vector of the first-stage decisions must be made before the scenario is known
$\boldsymbol{y}_s$	Vector of decisions made after the first stage, or as a result of the scenario realization

C. Parameters

β_{ch}, β_{dis}	Charging and discharging efficiencies of energy storage systems (ESSs)
γ^{ESS}	Recovery factor of ESSs
η_t	Electricity price during time t
θ	Power factor of ESSs
λ_{ij}	Failure rate of line (i,j)
$\lambda_{a,x,ij}$	Failure rate under weather condition a in year x of line (i,j)
$\tau_i(s)$	Load level uncertainty for a stochastic scenario, which is assumed to follow a normal distribution

Manuscript received: July 29, 2022; revised: November 17, 2022; accepted: December 19, 2022. Date of CrossCheck: December 19, 2022. Date of online publication: January 27, 2023.

This work was supported by National Natural Science Foundation of China (No. U1866603), Innovation Support Program of Chongqing for Preferential Returned Chinese Scholars (No. cx2021036), and Natural Science Foundation of Chongqing, China (No. CSTB2022NSCQ-BHX0729).

H. Chen, J. Wang (corresponding author), X. Xiong, and H. Yang are with State Key Laboratory of Power Transmission Equipment & System Security and New Technology, Chongqing University, Chongqing 400044, China (e-mail: chz0617@foxmail. com; wangrelay@foxmail. com; cquxxf@vip. sina. com; 20153326@cqu.edu.cn).

J. Zhu is with South China University of Technology, Guangzhou 510641, China (e-mail: zhujz@scut.edu.cn).

W. Wang is with the Electric Power Research Institute, State Grid Chongqing Electric Power Company, Chongqing 401123, China (e-mail: ww0326@outlook. com).

DOI: 10.35833/MPCE.2022.000467

$\Phi(s)$ Total annual operation cost of ADNs

ω_s Number of typical days throughout one year when scenario s is under normal, severe and extreme weather conditions

c_i^d Penalty cost for shedding load at node i

c_{ij}^h Annual cost for hardening distribution line (i,j)

c_{ij}^{sw} Annual cost for adding an automatic switch on line (i,j)

c^P, c^E Power and capacity costs of ESSs

c_{op} Annual operation-maintenance cost of per unit power capacity of ESS

C^h Total annual capital cost of hardening distribution lines

C^{sw} Total annual capital cost of upgrading automatic switches

C^{ESS} Total annual cost of deploying ESSs

C_{eq}^{ESS} Total annual equipment deployment cost of ESSs

C_{om}^{ESS} Total annual equipment operation-maintenance cost of ESSs

$E_{i,s,t}^{ESS}$ Energy capacity of ESS at the end of time t

M A large constant

N^{ESS} Limited investment of ESSs

n_{ij} Number of statistical years of line (i,j)

N_{ij} Number of failures of line (i,j)

$N_{a,x,ij}$ Number of failures of line (i,j) caused by weather condition a in year x

$p(s)$ Probability of occurrence of scenario s

P_{eq}^{ESS}, E_{eq}^{ESS} Rated power and capacity of ESSs

r_{ij}, x_{ij} Resistance and reactance of line (i,j)

$S_{ij,s,t}^{\max}$ Rated apparent power from node i to node j during time t in scenario s

SOC_{t_0} Initial state of charge of ESS

$SOC_{\min}$, $SOC_{\max}$ The minimum and maximum allowable states of charge

$T_{a,x}$ Duration of weather condition a in year x of the same historical period

$v_{i,s,t}$ Square of voltage magnitude at node i

$v_i^{\min}$, $v_i^{\max}$ Squares of lower and upper bound of allowable voltage magnitude at node i

D. Variables

$\alpha_{ij,s,t}$ A binary variable, which is equal to 1 if the state of line (i,j) is closed during time t in scenario s and 0 otherwise

$\eta_{ij,s,t}$ A binary variable, which is equal to 1 if the state of line (i,j) is damaged during time t in scenario s and 0 otherwise

μ_{ij,s,t_0} A binary variable, which is equal to 1 if line (i,j) is operating at time t_0 in scenario s and 0 otherwise

$\varphi_{ij,s,t}$ A binary variable, which is equal to 1 if the line switch on line (i,j) is closed during time t in scenario s and 0 otherwise

$\xi_{ij,s,t}^1$ A variable that represents the fault state of line (i,j) during time t in scenario s if it is hardened

$\xi_{ij,s,t}^0$ A variable that represents the fault state of line (i,j) during time t in scenario s if it is not hardened

F_{arb}^{ESS} Benefits of ESSs from peak shaving and valley filling

$I_{ij,s,t}$ Current of line (i,j) during time t in scenario s

$M^P(t)$, $M^Q(t)$ Active and reactive load curve values during time t

P_i, Q_i Reference values of active and reactive loads at node i

$P_{i,s,t}^{ch}$, $P_{i,s,t}^{dis}$ Active charging and discharging power of ESS at node i during time t in scenario s

$P_{ij,s,t}$, $Q_{ij,s,t}$ Active and reactive power flows from node i to node j during time t in scenario s

$P_{i,s,t}^g$, $Q_{i,s,t}^g$ Active and reactive power generated by distributed generator (DG) connected to node i during time t in scenario s

$P_i^{g,\max}$, $Q_i^{g,\max}$ Upper bounds of active and reactive power of DG connected to node i

$P_{i,s,t}^d$, $Q_{i,s,t}^d$ Actual active and reactive loads at node i during time t in scenario s

$P_{i,s,t}^c$, $Q_{i,s,t}^c$ Active and reactive load sheddings at node i during time t in scenario s

$Q_{i,s,t}^{ch}$, $Q_{i,s,t}^{dis}$ Reactive charging and discharging power of ESS at node i during time t in scenario s

$u_{i,s,t}^{ESS,ch}$, $u_{i,s,t}^{ESS,dis}$ Binary variables, which are equal to 1 if ESS is charging or discharging during time t in scenario s and 0 otherwise

x_{ij}^h A binary variable, which is equal to 1 if line (i,j) is hardened and 0 otherwise

$x_{ij}^{sw_0}$ A binary variable, which is equal to 1 if line (i,j) has an existing switch and 0 otherwise

$x_{ij}^{sw_1}$ A binary variable, which is equal to 1 if new line switch is added on line (i,j) and 0 otherwise

x_{ij}^{sw} A binary variable, which is equal to 1 if line (i,j) has switch and 0 otherwise

x_i^{ESS} A binary variable, which is equal to 1 if ESS is connected to node i and 0 otherwise

I. Introduction

In recent years, the frequent occurrence of extreme weather events has battered the power system, causing customers to experience different degrees of power outages after damaging the power grid infrastructure, and resulting in enormous economic losses [1]. In 2017, the hurricane Irma led to a power outage of 6.7 million electricity customers that account for 67% of all state customers in Florida [2]. In February 2021, a large-scale blackout occurred in Texas for

four days due to the influence of a snowstorm [3]. Unfortunately, the frequency and intensity of extreme weather events such as floods, hurricanes, and forest fires are forecasted to increase with the acceleration of climate change [4]. Most of the distribution networks are designed according to the meteorological conditions of a particular return period, i.e., 50 years, hence, they cannot withstand the damage caused by extreme weather events [5]. In order to effectively mitigate the impact of various extreme weather events, it is necessary to upgrade and update the distribution network considering random scenarios referring to different operation states of active distribution networks (ADNs) caused by meteorological disaster events.

As the ADN is still vulnerable to natural disasters, ensuring the rapidity and effectiveness of fault restoration has become a research priority in the power industry [6]. After disastrous weather, the restoration time of ADNs depends on rapid and accurate assessment of system damage. At present, the ADN usually dispatches inspectors to assess the degree of damage and the necessary materials for repairing. If an ADN is not fully prepared and lacks situation awareness [7], the restoration process will be seriously delayed, and customers will experience long-term power outages, which will cause national economic loss. As a result, researchers in academia and industry have jointly proposed the concept of resilience, that is, the ability of ADNs to prevent and adapt to environmental changes, withstand disturbances (including deliberate attacks, accidents, and natural disasters), and quick restoration [8]. In addition, resilience enhancement can be achieved by minimizing outage duration and maximizing restored load [9]. The resilience enhancement goals also can be fulfilled through upgrading and operating measures. For example, hardening line makes it less likely to be damaged in disaster. Upgrading automatic switches can quickly redistribute power to customers and shorten their outage time by network reconfiguration [10]. Energy storage system (ESS) provides a wide range of applications and additional operational flexibility for ADNs to enhance recovery capability in emergency situations. In general, enhancing the resilience of ADNs can be divided into 4 stages: planning stage (PLS), preventive response stage (PRS), emergency response stage (ERS), and restoration stage (RTS) [11]. This paper focuses on the two-stage programming model for the allocation of emergency resources.

In the PLS, taking precautionary measures such as hardening lines [12], managing vegetation [13], and deploying distributed power sources [14] for critical power assets can improve the robustness of distribution networks and the availability of emergency resources. In the ERS, loads can be restored by the real-time responsive strategies based on the available resources. Reference [15] presents a new three-stage resilience-driven framework for hardening power distribution systems to determine the capacity and location of the ESS for enhancing resilience against earthquakes. Reference [16] proposes a two-stage stochastic mixed-integer linear programming (SMILP) to optimize the preparation and resource allocation process for upcoming extreme weather events, which leads to faster and more efficient post-event restoration. However, most of these studies focus on planning for extreme scenarios only, lacking a comprehensive consideration of multiple scenarios. And the conventional model [17] neglects the issue of multi-stage problem and does not reflect the temporal feature of ESSs in the PLS. Due to energy storage that has strong time coupling constraints and is more complex to model, single-stage planning, which lacks an integrated layout of long-term investment strategies, can easily lead to over-investment and idle assets if these factors are not taken into account.

In contrast, the two-stage programming divides the planning cycle into different stages and solves the optimal solution of the model according to the growth of different factors during the planning cycle. For the two-stage programming problem of enhancing the resilience of ADNs, more uncertainties in distribution lines and loads caused by disastrous weather events need to be considered. Considering the shorter time scale of the emergency support process compared with the restoration process, uncertainties in the operation state of lines, the load level and the initial charge state of ESSs can all have impacts on the outcome of dispatch implementation. Robust optimization and stochastic programming models are widely used. In terms of robust optimization, [18] proposes to utilize the measures of hardening distribution lines and allocating energy storage to enhance the resilience of distribution networks against natural disasters. Reference [13] establishes a three-level robust optimization model considering the upgrading tower, managing vegetations, and their combination. The calculation burdens of the models in the above literature are relatively small, but the optimization results are too conservative due to the small probability of the worst case. In addition, important measures for strengthening grid such as automatic switches and emergency power supply are ignored. In terms of stochastic programming, a two-stage stochastic mixed-integer model is established and solved by utilizing the progressive hedging algorithm (PHA) considering hardening distribution line, upgrading automatic switch, and deploying distributed generator (DG) in [12]. However, the number of variables involved in the above model leads to a more complex model, and the scale of DG is not considered.

At present, the planning problem with a single stage or a certain scenario is generally a small-scale stochastic mixed-integer programming (SMIP) model, which can be directly solved by optimization solvers such as Yalmip or Gurobi. The multi-stage planning problem is generally a large-scale SMIP model, which is difficult to directly call the solver to calculate. Robust optimization is generally solved by Benders decomposition algorithm or column-and-constraint generation (C&CG) algorithm. The primal problem is decomposed into the main problem and the sub-problem to obtain the optimal solution of the primal problem alternately [19]. The two-stage stochastic programming model has discrete decision variables in the first and second stages, which cannot be solved by the Benders decomposition algorithm. The PHA is usually used to solve the SMIP problem. The primal problem is divided into sub-problems based on the scenario, and the sub-problems are solved in parallel, thus reducing the computational difficulty. PHA can be adopted as a heuristic to ensure the convergence and efficiency of the model in

the presence of discrete decision variables [20].

Therefore, in order to enhance the resilience of ADNs, this paper establishes a two-stage SMIP model to minimize the upgrading and operation cost of ADNs by considering random scenarios referring to different operation states of ADNs. In the first stage, the system planner makes investment decisions: hardening existing distribution lines, upgrading automatic switches, and deploying energy storage resources. The second stage is to evaluate the operation cost of ADNs to ensure the supply of loads after network reconfiguration during meteorological disasters and the optimal utilization of ESSs in different scenarios. Besides, a new modeling method is proposed to address the uncertainty of operation state of distribution lines. Based on historical statistics, multiple representative scenarios are generated by Latin hypercube sampling, and the similar scenarios are reduced by adopting a K-means clustering method. The PHA is used to solve the proposed model. The contributions of this paper are outlined below.

1) The best access point of the ESS in different operation scenarios are comprehensively considered to exert its value as much as possible by dividing the operation scenarios of ADNs into normal, severe, and extreme weather conditions. In normal scenarios, the ESS is used to improve the operation economics of ADNs. During the fault recovery period, the ESS is considered as the emergency power supply to the critical loads through network reconfiguration; and in the PLS, the safety support of ESSs is played combining with the results of the risk assessment of ADNs. Compared with existing planning models that only consider extreme scenarios, the proposed model not only enhances the resilience of ADNs during meteorological disasters, but also balances safety and economy.

2) In the proposed model, a modelling method for describing the uncertainty of the operation state of distribution lines is constructed to handle the logical constraints among variables such as the initial state of distribution lines, the existence of automatic switches on the line, the state of switches, and the fault state of lines in a certain scenario. The proposed method reduces the multivariate coupled problem of operation state of distribution lines to a linear model in a canonical representation, which makes the proposed model simpler and easier to solve.

The remainder of this paper is organized as follows. Section II classifies the operation scenarios of ADNs. Section III describes the two-stage SMIP model. Section IV generates the scenarios of ADNs and introduces the solution algorithm of the proposed model. Section V utilizes the modified IEEE 33-node test system to verify the proposed model. Finally, Section VI concludes this paper.

II. Operation Scenarios of ADNs

For the operation analysis of ADNs, the short-term risk level in the future is often predicted by obtaining the external operation environment information and combining with the operation parameters of lines, which is called predictive evaluation. For the planning analysis, the estimated value can be obtained after the data from long-term operation records are analyzed, which is called statistical analysis. In this paper, the ESS is applied to the planning model to improve the flexibility of the ADN, and historical statistical data are applied to the typical operation scenarios of the ADN to simplify the failure rate model [21].

The main causes for the failure of ADNs are insulation damage, external force damage, and natural disasters. Among natural disasters, mountain fires, thunderstorms, and typhoon have greater impacts on ADNs. Therefore, this paper divides the operation scenarios of ADNs into normal, severe, and extreme weather conditions. ADN is in a normal operation state under normal weather condition, and in a fault operation state in response to meteorological disasters under severe and extreme weather conditions. Different operation states of ADNs throughout the year for comprehensive planning are considered in this paper.

A. Participation of ESSs Under Normal Weather Condition

The energy storage technologies currently used in power grids can be divided into four categories: electrical energy storage, mechanical energy storage, chemical energy storage, and thermal energy storage [22]. Battery energy storage, which has the advantages of high efficiency, fast response speed, and low maintenance cost, has become one of the most promising energy storage technologies [23]. The major drawback of other energy storage technologies lies in the scarcity of available sites and low energy density. So, the demand for battery energy storage has gradually increased in the market due to the advances in battery manufacturing technology and improvements in battery life and cost issues [24]. Therefore, this paper chooses battery energy storage as the research object.

ESS can effectively realize the conversion, storage, and utilization of electrical energy, and it is a kind of critical means to improve the flexibility, economy, and safety of the power grid [25]. By absorbing and injecting electrical energy into ADNs, the ESS has the advantages of regulating voltage, peak shaving and valley filling, and decreasing network loss. The mismatch between the load demand and the real-time balance demand of power generation and load is alleviated. By reasonably adjusting the charging/discharging operation mode of the ESS, it can effectively compensate for the mismatch between distributed generation output and load demand of ADNs, and alleviate the real-time balance demand between generation and load.

To simplify the model, this paper mainly considers the benefits of the ESS from peak shaving and valley filling under normal weather condition:

$$F_{arb}^{ESS}=\sum_{t\in T}\eta_t\sum_{i\in N}(P_{i,s,t}^{dis}-P_{i,s,t}^{ch})\Delta t \tag{1}$$

B. Participation of ESSs Under Severe and Extreme Weather Conditions

Under meteorological disasters, the resistance and recovery process of the ADN [26], as shown in Fig. 1, can be divided into the following stages. The first stage (0-t_e) represents resilient state before the disaster. The second stage (t_e-t_{pe}) represents event progress, during which the ADN is affected by extreme disasters and large-scale power outages are gradually caused. The third stage (t_{pe}-t_r) represents post-

event degraded state, and the ADN is in the preparation state after the disaster occurs and before the ADN takes recovery measures. In this stage, the ADN may be completely out of power. It may also rely on itself to maintain power supply to part of loads, and the ADN is ready for emergency recovery. The fourth stage (t_r-t_{pr}) represents restorative state, which is a stage for the system to take emergency measures to restore critical loads first. In this stage, according to the importance of load, various resources are coordinated to restore the power supply to the loads, so as to reduce the impact on society. The fifth stage (t_{pr}-t_{ir}) represents infrastructure recovery state. In this stage, according to the restoration plan, the damaged power distribution equipment is gradually repaired, the infrastructure restoration is carried out, and finally the complete recovery of the load is realized.

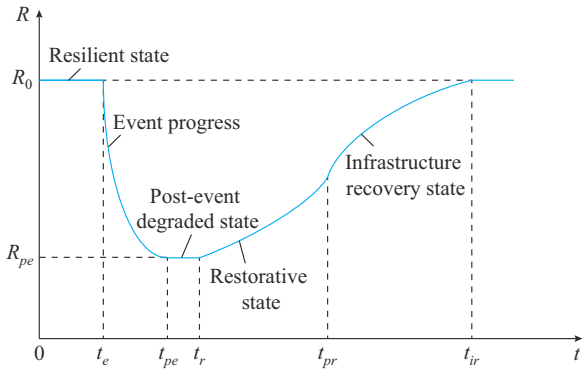

Fig. 1. Resistance and recovery process of ADN.

There are two special problems of ESS planning when considering the meteorological disasters. First, compared with distributed power generation, ESS planning has strong time coupling constraints, so its modeling is more complex. Second, the limited investment budget will limit the extensive allocation of ESSs. An ESS can provide a short-term emergency response to pick up the load and reduce economic losses during the fourth stage. After an ADN enters infrastructure recovery, the grid maintenance personnel will take recovery measures such as transferring supply, and ESSs may not be able to continue discharging due to its own capacity limitations, so this paper only considers the participation of ESSs in the emergency response state.

Aiming at responsiveness and catastrophic severity in different states during the resilience recovery process, the evaluation index, i.e., load loss rate (LLR) [8], is employed to reflect the resilience of distribution networks, as shown in (2). It is the integral of the declining part of the resilience index and the time axis between t_e and t_{pr}. In other words, the greater the ability of ADNs to recover quickly after a disaster, the greater the resilience and the smaller the LLR.

$$LLR=\int_{t_e}^{t_{pr}}\sum_{i\in N}c_i^d P_{i,s,t}^c \mathrm{d}t \approx \sum_{t\in T}\sum_{i\in N}c_i^d P_{i,s,t}^c \Delta t \tag{2}$$

III. Two-stage SIMP Model

A. Objective Function

The objective of this paper is to improve the benefits of ESSs in terms of peak shaving and valley filling and to reduce the cost following two aspects: ① investment cost of hardening distribution lines, upgrading automatic switches, and deploying ESSs; and ② the cost of load shedding in response to extreme disasters during the emergency period.

Correspondingly, the objective function of the planning model (in unit of year) is as follows:

$$\min\{C^h+C^{sw}+C^{ESS}+\Phi(s)\} \tag{3}$$

$$C^h=\sum_{(i,j)\in L}c_{ij}^h x_{ij}^h \tag{4}$$

$$C^{sw}=\sum_{(i,j)\in SW}c_{ij}^{sw}x_{ij}^{sw_1} \tag{5}$$

The cost of ESSs includes equipment deployment cost C_{eq}^{ESS} and annual operation maintenance cost C_{om}^{ESS}, as shown in (6)-(8). The equipment deployment cost of ESSs is related to the configured capacity and the maximum discharge power.

$$C^{ESS}=(1-\gamma^{ESS})C_{eq}^{ESS}+C_{om}^{ESS} \tag{6}$$

$$C_{eq}^{ESS}=\sum_{i\in N}(c^P P_{eq}^{ESS}+c^E E_{eq}^{ESS})x_i^{ESS} \tag{7}$$

$$C_{om}^{ESS}=\sum_{i\in N}c_{om}P_{eq}^{ESS}x_i^{ESS} \tag{8}$$

Since the operation conditions of ADNs are divided into different scenarios, the annual operation cost of ADNs is the lowest sum of the operation cost $C^D(s)$ in different scenarios, as shown in (9). The operation cost of ADNs in scenario s is the cost of load shedding minus the benefits of ESSs in terms of peak shaving and valley filling in (10).

$$\Phi(s)=\min\left\{\omega_s\sum_{s\in S}p(s)C^D(s)\right\} \tag{9}$$

$$C^D(s)=\sum_{t\in T}\sum_{i\in N}c_i^d P_{i,s,t}^c\Delta t-F_{arb}^{ESS} \tag{10}$$

B. Constraints

1) PLS Constraints

$$x_{ij}^{sw_0}+x_{ij}^{sw_1}=x_{ij}^{sw} \tag{11}$$

$$\sum_{i\in N}x_i^{ESS}\le N^{ESS} \tag{12}$$

2) Line Fault State Constraints

Based on the failure rate of historical statistics, the fault state of distribution lines in a scenario is obtained by sampling. It is worth noting that hardening existing distribution lines can only reduce the failure rate, but cannot fully ensure normal operation. To manage the risk in a more realistic way, when a line is hardened, the failure rate is assumed to be 1/10 of that before the hardening. The uncertainty of line fault state is decoupled by two independent parameters, which can be generated in advance to represent the line fault state weather it is hardened.

$$\eta_{ij,s,t}=(1-x_{ij}^h)\xi_{ij,s,t}^0+x_{ij}^h\xi_{ij,s,t}^1 \tag{13}$$

3) Logic Constraints

At present, most ADNs are not fully automated, that is, not all lines have automatic switches. In addition, the tie line of ADNs does not participate in the normal operation. The initial state of the distribution line, whether there is an auto-

matic switch on the line, and the fault state of the line in a certain scenario will affect the final operation state of the line, which makes it difficult to model the actual state of the line. In order to solve this problem, this paper establishes the logical relationship between variables, as shown in the Table I, and formulates the logical constraints, as shown in (14)-(19).

TABLE I
LOGICAL CONSTRAINTS BETWEEN VARIABLES

μ_{ij,s,t_0}	x_{ij}^{sw}	$\eta_{ij,s,t}$	$\varphi_{ij,s,t}$	$\alpha_{ij,s,t}$
1	1	1	0	0
		0	0	0
		0	1	1
	0	1		0
		0		1
0	1	1	0	0
		0	0	0
		0	1	1
	0	1		0
		0		0

$$\varphi_{ij,s,t} \le x_{ij}^{sw} \tag{14}$$

$$\varphi_{ij,s,t} + \eta_{ij,s,t} \le 1 \tag{15}$$

$$\alpha_{ij,s,t} - x_{ij}^{sw} M \le (1-\eta_{ij,s,t})\mu_{ij,s,t_0} \le \alpha_{ij,s,t} + x_{ij}^{sw} M \tag{16}$$

$$\alpha_{ij,s,t} - (1-x_{ij}^{sw})M \le \varphi_{ij,s,t} \le \alpha_{ij,s,t} + (1-x_{ij}^{sw})M \tag{17}$$

$$0 \le P_{i,s,t}^{c} \le P_{i,s,t}^{d} \tag{18}$$

$$0 \le Q_{i,s,t}^{c} \le Q_{i,s,t}^{d} \tag{19}$$

If a fault occurs on a normal line, the line will be out of service. If no fault occurs, the actual running state of the line is determined by the state of the line switch, i.e., if the switch is closed, the line is in operation, and if the switch is open, the line is out of service. If there is no switch on a normal line, the line is out of service when a fault occurs. The above results correspond to all cases ($\mu_{ij,s,t_0}=1$) in Table I. Lines with an initial state of non-operational ($\mu_{ij,s,t_0}=0$) have the same logical variables as normal lines in most cases. It is worth noting that a standby line without an automatic switch will not be in operation state even if no fault occurs, i.e., it cannot participate in emergency support. Constraint (14) represents that a line with an automatic switch is the only way to discuss whether the switch is closed or not. Constraint (15) represents that once a fault occurs on a line, the line with an automatic switch must be cut off. Constraint (16) represents that a normal line that does not have an automatic switch determines the final operation state by the fault state. Constraint (17) represents that the final operation state of a line with automatic switch is determined by the close or open state of the switch. Constraints (18) and (19) limit the upper and lower load cut limits, respectively.

4) Power Balance Constraints

$$\sum_{\forall(j,k)\in L} P_{jk,s,t} - \sum_{\forall(i,j)\in L}(P_{ij,s,t} - I_{ij,s,t}^2 r_{ij}) = P_{j,s,t}^{g} + P_{j,s,t}^{dis} - P_{j,s,t}^{ch} - (P_{j,s,t}^{d} - P_{j,s,t}^{c}) \tag{20}$$

$$\sum_{\forall(j,k)\in L} Q_{jk,s,t} - \sum_{\forall(i,j)\in L}(Q_{ij,s,t} - I_{ij,s,t}^2 x_{ij}) = Q_{j,s,t}^{g} + Q_{j,s,t}^{dis} - Q_{j,s,t}^{ch} - (Q_{j,s,t}^{d} - Q_{j,s,t}^{c}) \tag{21}$$

5) Transmission Capacity Constraints

$$P_{ij,s,t}^2 + Q_{ij,s,t}^2 \le \alpha_{ij,s,t} S_{ij,s,t}^{\max} \tag{22}$$

Since (22) is a nonlinear constraint, the linearization method [27] can be expressed as follows:

$$-\alpha_{ij,s,t} S_{ij,s,t}^{\max} \le P_{ij,s,t} \le \alpha_{ij,s,t} S_{ij,s,t}^{\max} \tag{23}$$

$$-\alpha_{ij,s,t} S_{ij,s,t}^{\max} \le Q_{ij,s,t} \le \alpha_{ij,s,t} S_{ij,s,t}^{\max} \tag{24}$$

$$-\sqrt{2}\,\alpha_{ij,s,t} S_{ij,s,t}^{\max} \le P_{ij,s,t} + Q_{ij,s,t} \le \sqrt{2}\,\alpha_{ij,s,t} S_{ij,s,t}^{\max} \tag{25}$$

$$-\sqrt{2}\,\alpha_{ij,s,t} S_{ij,s,t}^{\max} \le P_{ij,s,t} - Q_{ij,s,t} \le \sqrt{2}\,\alpha_{ij,s,t} S_{ij,s,t}^{\max} \tag{26}$$

6) Voltage Constraints

$$v_{i,s,t} - v_{j,s,t} \ge 2(r_{ij}P_{ij,s,t} + x_{ij}Q_{ij,s,t}) - (r_{ij}^2 + x_{ij}^2) I_{ij,s,t}^2 + (\alpha_{ij,s,t} - 1)M \tag{27}$$

$$v_{i,s,t} - v_{j,s,t} \le 2(r_{ij}P_{ij,s,t} + x_{ij}Q_{ij,s,t}) - (r_{ij}^2 + x_{ij}^2) I_{ij,s,t}^2 + (1-\alpha_{ij,s,t})M \tag{28}$$

$$v_i^{\min} \le v_{i,s,t} \le v_i^{\max} \tag{29}$$

7) Reconfiguration Constraints

$$\sum_{(j,i_r)\in L} f_{ji_r,s,t}^{k} - \sum_{(i_r,j)\in L} f_{i_r j,s,t}^{k} = -1 \quad \forall k \in N \backslash i_r \tag{30}$$

$$\sum_{(j,k)\in L} f_{jk,s,t}^{k} - \sum_{(k,j)\in L} f_{kj,s,t}^{k} = 1 \quad \forall k \in N \backslash i_r \tag{31}$$

$$\sum_{(j,i)\in L} f_{ji,s,t}^{k} - \sum_{(i,j)\in L} f_{ij,s,t}^{k} = 0 \quad \forall k \in N \backslash i_r, \forall i \in N \backslash \{i_r, k\} \tag{32}$$

$$\begin{cases} 0 \le f_{ij,s,t}^{k} \le \lambda_{ij,s,t} \\ 0 \le f_{ji,s,t}^{k} \le \lambda_{ji,s,t} \end{cases} \quad \forall k \in N \backslash i_r \tag{33}$$

$$\sum_{\forall(i,j)\in L} (\lambda_{ij,s,t} + \lambda_{ji,s,t}) = N - 1 \tag{34}$$

$$\lambda_{ij,s,t} + \lambda_{ji,s,t} = \beta_{ij,s,t} \tag{35}$$

$$\alpha_{ij,s,t} \le \beta_{ij,s,t} \tag{36}$$

Constraints (30) - (36) always ensure the radiality of the ADN, and a specific explanation can be found in [28].

8) Operation Constraints of DG

$$\begin{cases} 0 \le P_{i,s,t}^{g} \le P_i^{g,\max} \\ 0 \le Q_{i,s,t}^{g} \le Q_i^{g,\max} \end{cases} \tag{37}$$

9) Operation Constraints of ESSs

Constraint (38) limits the inability of ESSs to be charged and discharged simultaneously. Constraints (39) and (40) limit the charging and discharging rates of ESSs, respectively. Constraints (41) and (42) are the charging state constraints of ESSs. Constraints (43) and (44) are the reactive power constraints of ESSs. Constraint (45) limits the initial charging state of ESSs.

$$u_{i,s,t}^{ESS,ch} + u_{i,s,t}^{ESS,dis} \le x_i^{ESS} \tag{38}$$

$$0 \le P_{i,s,t}^{ch} \le u_{i,s,t}^{ESS,ch} P_{eq}^{ESS} \tag{39}$$

$$0 \le P_{i,s,t}^{dis} \le u_{i,s,t}^{ESS,dis} P_{eq}^{ESS} \tag{40}$$

$$E_{i,s,t}^{ESS} = E_{i,s,t-1}^{ESS} + \beta_{ch} P_{i,s,t}^{ch} - P_{i,s,t}^{dis}/\beta_{dis} \tag{41}$$

$$SOC_{\min} \cdot E_{eq}^{ESS} x_i^{ESS} \le E_{i,s,t}^{ESS} \le SOC_{\max} \cdot E_{eq}^{ESS} x_i^{ESS} \tag{42}$$

$$-\theta P_{i,s,t}^{ch} \le Q_{i,s,t}^{ch} \le \theta P_{i,s,t}^{ch} \tag{43}$$

$$-\theta P_{i,s,t}^{dis} \le Q_{i,s,t}^{dis} \le \theta P_{i,s,t}^{dis} \tag{44}$$

$$E_{i,s,t_0}^{ESS} = SOC_{t_0} \cdot E_{eq}^{ESS} x_i^{ESS} \tag{45}$$

SOC_{t_0} is 0.5 under normal weather condition. It is assumed that the SOC of ESSs can be adjusted before a disaster occurs.

10) Other Constraints

$$\varepsilon_{i,s,t} = 1 \quad \forall i \in \{N_r, N_g\} \tag{46}$$

$$\rho_{i,s,t} \ge \frac{1}{N^{ESS}+1} \sum_{i \in N} x_i^{ESS} \quad \forall i \in N \backslash \{N_r, N_g\} \tag{47}$$

$$\rho_{i,s,t} \le \sum_{i \in N} x_i^{ESS} \quad \forall i \in N \backslash \{N_r, N_g\} \tag{48}$$

$$\sigma_{i,s,t} \ge \frac{1}{M}\left(\sum_{(i,j) \in L} \varepsilon_{j,s,t} \alpha_{ij,s,t} + \sum_{(j,i) \in L} \varepsilon_{j,s,t} \alpha_{ij,s,t} \right) \quad \forall i \in N \backslash \{N_r, N_g\} \tag{49}$$

$$\sigma_{i,s,t} \le \sum_{(i,j) \in L} \varepsilon_{j,s,t} \alpha_{ij,s,t} + \sum_{(j,i) \in L} \varepsilon_{j,s,t} \alpha_{ij,s,t} \quad \forall i \in N \backslash \{N_r, N_g\} \tag{50}$$

$$\begin{cases} \varepsilon_{i,t} \ge \rho_{i,t} \\ \varepsilon_{i,t} \ge \sigma_{i,t} \\ \varepsilon_{i,t} \le \rho_{i,t} + \sigma_{i,t} \end{cases} \quad \forall i \in N \backslash \{N_r, N_g\} \tag{51}$$

Constraints (46)-(51) are energized constraints, and a specific explanation can be found in [29].

IV. Scenario Generation of ADNs and Solution Algorithm

Due to the uncertainty of faulty lines and load state, the SMIP model proposed in this paper is an optimization problem that contains all random scenarios. To ensure a balance between computational accuracy and efficiency, this paper first obtains fault probabilities of lines based on historical statistics, then adopts Latin hypercube sampling to generate representative operation scenarios, and finally uses K-means clustering to reduce the scenarios.

A. Scenario Generation

In this paper, a large number of scenarios of ADNs are generated by sampling. The scenario generation considers two uncertain factors.

1) Uncertainty of Load State

Based on historical statistical load data, the load data of typical days are selected as the base load profiles. Assume that all nodes adopt the same typical load curve, which can be expressed as follows:

$$P_{i,s,t}^{d} = \tau_i(s) M^{P}(t) P_i \tag{52}$$

$$Q_{i,s,t}^{d} = \tau_i(s) M^{Q}(t) Q_i \tag{53}$$

2) Line Failure Rate

The failure rates of ADNs are determined based on time and weather-dependent fault statistics [30]. Assuming that there are m lines of a certain voltage level, the calculation method of the distribution line failure rate [21] is shown in (54).

$$\lambda_{ij} = \frac{N_{ij}}{L_{ij} n_{ij}} \tag{54}$$

The calculation method of typical daily failure rate under different weather conditions is as follows:

$$\lambda_{a,x,ij} = \frac{365}{T_{a,x}} \frac{N_{a,x,ij}}{L_{ij}} \tag{55}$$

After calculating $\lambda_{a,x,ij}$, the fault state of the line is obtained according to the sampling result. That is, if a random number between 0 and 1, i.e., $U(0,1) \le \lambda_{a,x,ij}$, $\xi_{ij,s,t}^{0} = 1$, otherwise, $\xi_{ij,s,t}^{0} = 0$; if $U(0,1) \le 0.1\lambda_{a,x,ij}$, $\xi_{ij,s,t}^{1} = 1$, otherwise, $\xi_{ij,s,t}^{1} = 0$.

B. Scenario Reduction

Among the scenarios generated by sampling, the number of some scenarios is small while the number of other scenarios is large. First, the failure rate of lines is low under normal weather condition, so most of normal scenarios are exactly the same. Second, the fault locations in severe and extreme scenarios may be the same, and even if the fault locations are different, the unsupplied loads obtained by the second-stage optimization are close to each other. Therefore, this paper adopts K-means clustering to reduce the scenarios [31].

The unsupplied load $\Delta C_i^D(s)$ at node i can be obtained by solving the two-stage problem in scenario s, as shown in (56). Then, the unsupplied load vector $\Delta \boldsymbol{C}^D(s)$ can be expressed as (57).

$$\Delta C_i^D(s) = \sum_{t \in T} P_{i,s,t}^{c} \Delta t \tag{56}$$

$$\Delta \boldsymbol{C}^D(s) = [\Delta C_1^D(s) \quad \Delta C_2^D(s) \quad \cdots \quad \Delta C_N^D(s)] \tag{57}$$

K-means clustering aims to partition the N_S-dimensional vector $[\Delta \boldsymbol{C}^D(1), \Delta \boldsymbol{C}^D(2), ..., \Delta \boldsymbol{C}^D(N_S)]$ into k ($k<N_S$) sets $\psi_1, \psi_2, ..., \psi_k$ so as to minimize the within-cluster sum of distance $\sigma(k)$:

$$\sigma(k) = \arg\min \sum_{i=1}^{k} \sum_{\Delta \boldsymbol{C} \in \psi_i} \left\| \Delta \boldsymbol{C} - \boldsymbol{\mu}_i \right\|^2 = \arg\min \sum_{i=1}^{k} \left| \psi_i \right| \cdot Var(\psi_i) \tag{58}$$

$Var(\cdot)$ is the function of calculating variance. After the clustering, if a set ψ_i contains multiple scenarios, one scenario among ψ_i can be randomly selected. The probability of this representative scenario $\hat{p}(\omega)$ is the sum of all scenarios within this cluster:

$$\hat{p}(\omega) = \sum_{s \in \varphi_i} p(s) \tag{59}$$

$$p(s) = 1/N_S \tag{60}$$

$$\sigma(k_0) - \sigma(k_0 + 5) < 0.2(\sigma(k_0 - 5) - \sigma(k_0)) \tag{61}$$

The value of k is 20-40 with a step of 5. When k satisfies (61), k_0 be regarded as a proper value because it indicates that $\sigma(k)$ begins to saturate. Eventually, the reduced k scenarios are fed back into the SMIP problem.

C. PHA

The two-stage SMIP model established in this paper can be expressed as follows:

$$\min_{x}\left\{\boldsymbol{c}^{\mathrm{T}}\boldsymbol{x}+\sum_{s\in S}p(s)(\boldsymbol{f}_s^{\mathrm{T}}\boldsymbol{y}_s)\right\} \tag{62}$$

s.t.

$$(\boldsymbol{x},\boldsymbol{y}_s)\in\mathcal{Q}_s \quad \forall s\in\mathcal{S} \tag{63}$$

$\boldsymbol{x}$ implicitly implements the non-anticipative constraints that avoid allowing decisions to depend on the scenario. By introducing copies of $\boldsymbol{x}$, the block-angular structure leads to the so-called scenario formulation of the SMIP model:

$$\min_{x}\sum_{s\in S}p(s)(\boldsymbol{c}^{\mathrm{T}}\boldsymbol{x}+\boldsymbol{f}_s^{\mathrm{T}}\boldsymbol{y}_s) \tag{64}$$

s.t.

$$\begin{cases}(\boldsymbol{x},\boldsymbol{y}_s)\in\mathcal{Q}_s\\ \boldsymbol{x}(1)=\boldsymbol{x}(2)=\ldots=\boldsymbol{x}(N_s)\end{cases}\quad\forall s\in S \tag{65}$$

$\boldsymbol{x}(1)=\boldsymbol{x}(2)=\ldots=\boldsymbol{x}(N_s)$ represents the non-anticipative constraint, which guarantees the first-stage decision vector $\boldsymbol{x}$ independent of scenarios. Finally, this scenario formulation ((64) and (65)) decomposes the large-scale SMIP problem into scenario subproblems with the non-anticipative constraints. The PHA is used to solve the large-scale SMIP problem due to the uncertainty of multi-scenario. The steps are as follows.

Step 1: $k=0$.

Step 2: for all $s\in S$, $\boldsymbol{x}_s^{(k)}:=\arg\min_{\boldsymbol{x},\boldsymbol{y}_s}(\boldsymbol{c}^{\mathrm{T}}\boldsymbol{x}+\boldsymbol{f}_s^{\mathrm{T}}\boldsymbol{y}_s):(\boldsymbol{x},\boldsymbol{y}_s)\in\mathcal{Q}_s$.

Step 3: $\bar{\boldsymbol{x}}^{(k)}=\sum_{s\in S}p(s)\boldsymbol{x}_s^{(k)}$.

Step 4: for all $s\in S$, $\boldsymbol{w}_s^{(k)}=\rho(\boldsymbol{x}_s^{(k)}-\bar{\boldsymbol{x}}^{(k)})$.

Step 5: $k=k+1$.

Step 6: for all $s\in S$, $\boldsymbol{x}_s^{(k)}=\arg\min_{\boldsymbol{x},\boldsymbol{y}_s}(\boldsymbol{c}^{\mathrm{T}}\boldsymbol{x}+\boldsymbol{w}_s^{(k-1)}\boldsymbol{x}+\rho/(2\|\boldsymbol{x}-\bar{\boldsymbol{x}}^{(k-1)}\|^2)+\boldsymbol{f}_s^{\mathrm{T}}\boldsymbol{y}_s):(\boldsymbol{x},\boldsymbol{y}_s)\in\mathcal{Q}_s$.

Step 7: $\bar{\boldsymbol{x}}^{(k)}=\sum_{s\in S}p(s)\boldsymbol{x}_s^{(k)}$.

Step 8: for all $s\in S$, $\boldsymbol{w}_s^{(k)}=\boldsymbol{w}_s^{(k-1)}+\rho(\boldsymbol{x}_s^{(k)}-\bar{\boldsymbol{x}}^{(k)})$.

Step 9: $g^{(k)}=\sum_{s\in S}p(s)\|\boldsymbol{x}_s^{(k)}-\bar{\boldsymbol{x}}^{(k)}\|$.

Step 10: if $g^{(k)}<\epsilon$, where ϵ is the termination threshold, go to *Step 5*; otherwise, terminate.

The size of ρ in the PHA directly affects the convergence and solution speed of the model [32]. In this paper, ρ is set to be proportional to the unit cost of the decision variable [33].

V. Case Study

The test is conducted based on the modified IEEE 33-node test system to verify the validity of the proposed model, using MATLAB R2018b with YALMIP toolbox on a computer with an Intel Core i5-8400 processor and 16 GB of memory. The SMIP model is solved by Gurobi 9.5.1. The mixed-integer programming (MIP) gap is set to be 1%. The single time span is set to be 15 min.

A. Modified IEEE 33-node Test System

The modified IEEE 33-node test system is shown in Fig. 2. The system reference capacity is 10 MVA, and the reference voltage is 12.66 kV. The allowable range of node voltage is 0.9 to 1.1 p.u.. A DG with an output range of 0 to 0.5 MW is connected to node 2. It is assumed that the life time of the three measures (hardening distribution lines, upgrading automatic switches, and deploying ESSs) is 10 years. Without considering interest rates, the annual capital cost of purchasing and deploying each measure is 1/10 of the initial investment cost. The span of two consecutive poles is 50 m [13]. The basic load shedding cost is 100 ¥/kWh, and the weight is generated by a random number. The critical load shedding penalty cost is much higher, which is set to be 1000 ¥/kWh [34]. The maximum rated power and capacity of the ESS deployed are 300 kW and 600 kWh, respectively. The maximum number of ESSs allowed to be deployed in ADNs is 6, the discharge efficiency is 0.9, and the range of SOC is 0.05 to 0.95. The recovery factor of ESSs is 0.2. Other parameters are shown in Table II.

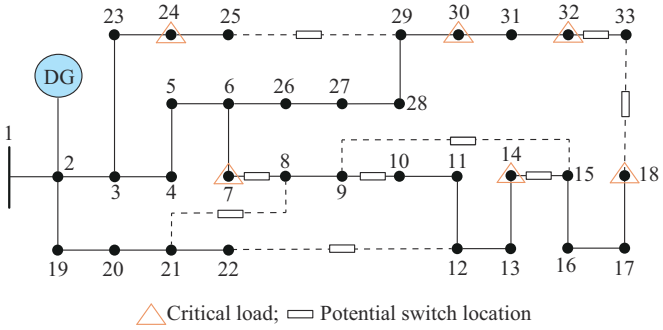

Fig. 2. Modified IEEE 33-node test system.

TABLE II
Positions and Cost of Different Measures

Measure	Candidate position	Value
Hardening lines	All line sections	c_{ij}^{h}=¥42000
Upgrading automatic switches	Pre-selected lines	c_{ij}^{sw}=¥106000
Deploying ESSs	All nodes	c^{P}=800 ¥/kW, c^{E}=1005 ¥/kWh, c_{op}=64 ¥/kW

B. Experiment Results

1) Scenario Generation and Reduction

It is assumed that there are 300 typical days of normal weather condition, 10 occurrences of severe weather condition, and 5 occurrences of extreme weather condition throughout the year. Each occurrence of the severe and extreme weather conditions may last for 1 to 3 days. Since this paper discusses the emergency response period under disastrous weather conditions, a typical day is considered to represent the severe and extreme weather conditions, respectively. Besides, the emergency period is assumed as 2 hours during a fault.

The load curves of each typical day under different weather conditions are shown in Fig. 3, and the time-of-use tariff for customers is shown in Table III. We use thunderstorm weather to represent severe weather and use typhoon to represent extreme weather. The failure rate in thunderstorm weather is shown in Appendix A Table AI, which is from the annual statistics [35] of a certain area in southern China. The failure rates of distribution lines in typhoon weather are

obtained from the statistical value of a certain region [36]. After obtaining the failure rate of each distribution line, the fault states of the lines are determined by Latin hypercube sampling.

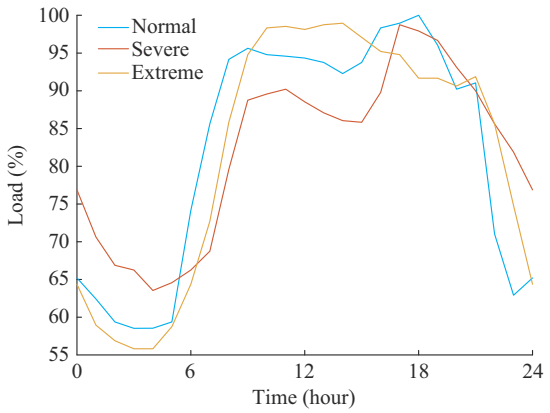

Fig. 3. Typical load curves of each typical day under different weather conditions.

TABLE III
TIME-OF-USE TARIFF FOR CUSTOMERS

Session	Time	Tariff (¥/kWh)
1	00:00-08:00	0.3377
2	08:00-14:00 17:00-19:00 22:00-24:00	0.6648
3	14:00-17:00 19:00-22:00	1.0900

Since the number of scenarios for solving the proposed SMIP model should be at least 50 [13], this paper generates 50 random scenarios for normal weather, severe weather, and extreme weather, respectively. The number of faulty lines in different scenarios is shown in Table IV.

TABLE IV
NUMBER OF FAULTY LINES IN DIFFERENT SCENARIOS

Normal weather		Severe weather		Extreme weather	
Number of scenarios	Number of faulty lines	Number of scenarios	Number of faulty lines	Number of scenarios	Number of faulty lines
32	0	8	2	7	7
18	1	10	3	9	8
		14	4	13	9
		13	5	11	10
		4	6	9	11
		1	7	3	12

As failure rates of distribution lines are low under normal weather condition, there is no faulty line in most scenarios. Even if a fault occurs on the line, the ADN could operate normally by operating the automatic switch to disconnect the fault and resupply the load, so 50 scenarios under normal weather condition are simplified into one scenario, i.e., the normal operation of the ADN in a typical day (24 hours). However, the number of faulty lines is large under severe and extreme weather conditions, and the ADN cannot solve the load shedding problem by itself, so ESSs can be considered for emergency support. But considering the capacity limitation of ESSs, this paper only considers the emergency response period before grid maintenance.

After 50 failure scenarios for severe and extreme weather conditions are clustered, respectively, the sensitivity of within-cluster sum of distance $\sigma(k)$ for different distances k is shown in Fig. 4. Then, the numbers of representative failure scenarios of severe and extreme weather conditions are 25 and 30, respectively.

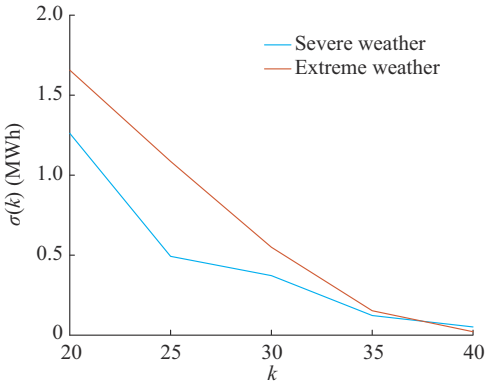

Fig. 4. Sensitivity of within-cluster sum of distance.

2) Planning Result

The penalty factor ρ of PHA is set to be 10000, being slightly smaller than c_{ij}^{sw}. After 87 iterations, the planning results of the proposed method are successfully obtained, as shown in Table V and Fig. 5.

TABLE V
PLANNING RESULTS OF PROPOSED METHOD

Cost (¥)			Cost of load shedding (¥)	Benefit of ESSs (¥)
Hardening lines	Upgrading automatic switches	Deploying ESSs		
840000	42400	519840	205977	1092711

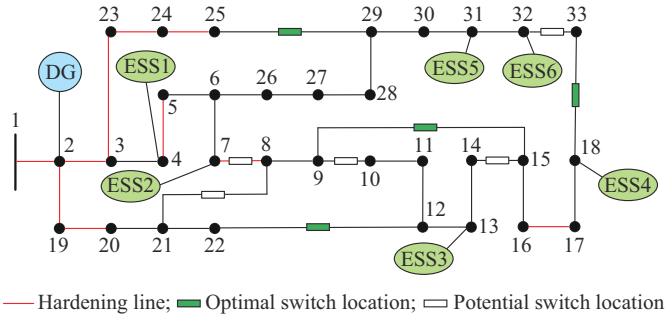

Fig. 5. Optimal results of proposed method.

The results show that the first measure involves an investment cost of ¥840000 to harden distribution lines $L_{1\text{-}2}$, $L_{2\text{-}3}$, $L_{4\text{-}5}$, $L_{7\text{-}8}$, $L_{16\text{-}17}$, $L_{2\text{-}19}$, $L_{19\text{-}20}$, $L_{3\text{-}23}$, $L_{23\text{-}24}$, and $L_{24\text{-}25}$; the second measure involves an investment cost of ¥42400 to deploy au-

tomatic switches on $L_{9\text{-}15}$, $L_{12\text{-}22}$, $L_{18\text{-}33}$, and $L_{25\text{-}29}$; and the third measure involves an investment cost of ¥519840 to deploy ESSs at nodes 4, 7, 13, 18, 31, and 32. Over the course of a year, the third measure benefits ¥1092711 through peak shaving and valley filling under the normal weather condition. Due to disastrous weather conditions, the number of faulty lines is higher, so even though the investment cost is higher, the emergency supply of load needs to be picked up as much as possible after the lines are hardened and automatic switches are upgraded. After the three measures are planned, the cost of load shedding for the year is ¥205977.

Figure 6 shows the planning results of structures involving reconfiguration during the failure period for scenario-9 under severe weather condition and scenario-16 under extreme weather condition.

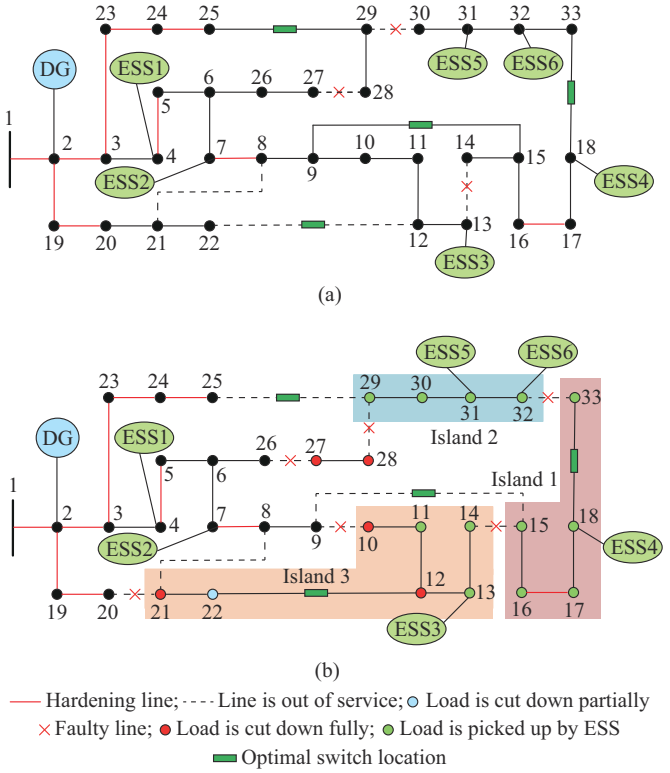

Fig. 6. Planning results of structures involving reconfiguration during failure period for scenario-9 and scenario-16. (a) Scenario-9 under severe weather condition. (b) Scenario-16 under extreme weather condition.

In scenario-9, $L_{2\text{-}3}$ and $L_{19\text{-}20}$ are no longer faulty after line hardening, only $L_{13\text{-}14}$, $L_{27\text{-}28}$, and $L_{29\text{-}30}$ are faulty, and the automatic switches on lines $L_{25\text{-}29}$, $L_{9\text{-}15}$, and $L_{18\text{-}33}$ have been upgraded and are able to close quickly to participate in the operation of the distribution network, so that all loads are recovered. In scenario-16, $L_{2\text{-}19}$, $L_{3\text{-}23}$, and $L_{24\text{-}25}$ are no longer faulty after line hardening, but there are still 6 lines, i. e., $L_{9\text{-}10}$, $L_{14\text{-}15}$, $L_{20\text{-}21}$, $L_{26\text{-}27}$, $L_{28\text{-}29}$, and $L_{32\text{-}33}$, that are faulty and the automatic switches on $L_{12\text{-}22}$ and $L_{18\text{-}33}$ are closed and eventually most of the loads are recovered. It can be observed from Fig. 6 that three isolated islands of the ADN are formed. The load is recovered by ESS4 at nodes 15, 16, 17, 18, and 33 in island 1, the load is recovered by ESS5 and ESS6 at nodes 29, 30, 31, and 32 in island 2, and the load is recovered by ESS3 at nodes 11, 13, 14, and 22 in island 3. The load at nodes 10, 12, and 21 is cut down. Due to the capacity limitation of ESS3, it is no longer able to continually provide enough power supply at node 22. The SOC of ESS3 in scenario-16 is shown in Fig. 7, which reflects the need for large-scale energy storage applications in a way to further improve the security of the distribution network. In summary, the planning results can ensure the ADN operates normally under most of severe weather conditions, and recover most of the loads under extreme weather conditions and avoid further economic losses.

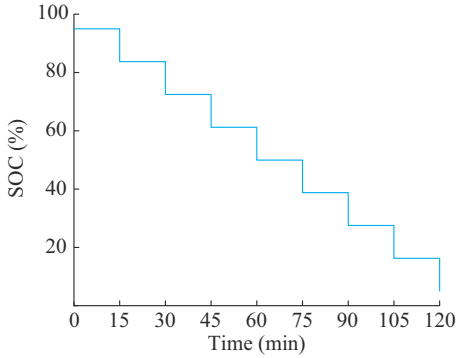

Fig. 7. SOC of ESS3 in scenario-16.

3) Comparison of Different Cases

Case 1: only hardening distribution lines and upgrading automatic switches without ESSs.

Case 2: hardening distribution lines and upgrading automatic switches responding to extreme weather condition, and deploying ESSs only at critical load nodes.

Case 3: using the proposed method, i.e., considering hardening distribution lines, upgrading automatic switches, and deploying ESSs.

The optimal planning results of the three cases are shown in Table VI. And the optimal planning results of Case 1 are shown in Fig. 8.

TABLE VI
OPTIMAL PLANNING RESULTS OF DIFFERENT CASES

Case	Objective	Cost (¥)			Cost of load shedding (¥)	Benefit of ESSs (¥)
		Hardening lines	Upgrading automatic switches	Deploying ESSs		
1	2463256	2184000	53000		186256	
2	794794	924000	53000	433200	295186	910592
3	515506	840000	42400	519840	205977	1092711

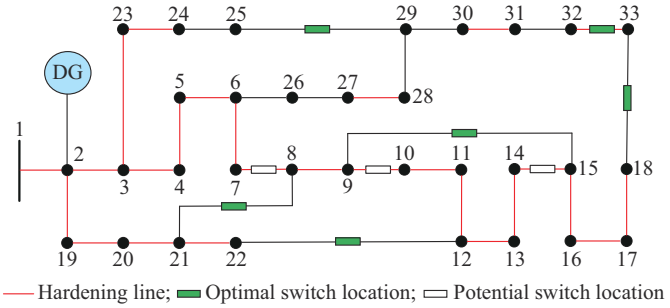

Fig. 8. Optimal planning results of Case 1.

It can be observed that if only hardening distribution lines and upgrading automatic switches are considered, although the cost of load shedding can be effectively reduced and the resilience of the ADN can be enhanced, the overall investment cost is larger without ESSs. Therefore, the planning results are less economical. The optimal planning results of Case 2 are shown in Fig. 9. It can be observed that the planning costs are still larger compared with the proposed method. ESSs are deployed only at critical load nodes 7, 14, 18, 30, and 31, which results in not only less benefit under the normal weather condition, but also more non-critical loads being cut down under disaster conditions, resulting in larger load cutting costs. With a comprehensive consideration of normal, severe, and extreme weather conditions, reasonable planning of hardening lines, upgrading automatic switches, and deploying ESSs can further reduce the cost of load shedding and ensure the benefit of ESSs while coordinating the safety of ADNs.

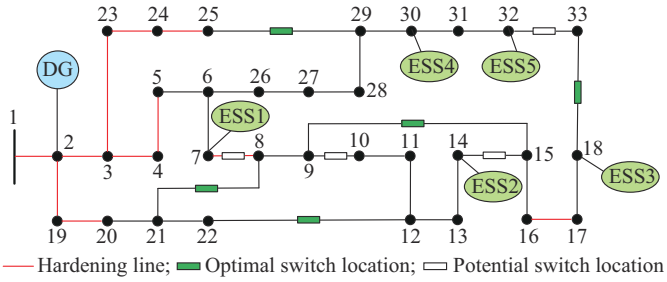

Fig. 9. Optimal planning results of Case 2.

VI. Conclusion

This paper proposes a novel two-stage SMIP model to enhance the resilience of ADNs in view of the fact that the existing distribution network is not able to withstand the damage caused by disastrous weather events. The first stage is to make decisions according to the measures of hardening existing distribution lines, upgrading automatic switches, and deploying ESSs. The second stage is to evaluate the operation cost of ADNs considering the cost of load shedding due to disastrous weather and the benefits of ESSs under different weather conditions. Logical constraints are formulated among variables such as the initial state of distribution lines, the existence of automatic switches on the line, the state of switches, and the fault state of lines in a certain scenario to portray the actual operation state of the line. This paper divides the year-round operation environment of ADNs into normal, severe, and extreme weather conditions. As an important resource to participate in enhancing the resilience of ADNs, the ESS can benefit from peak shaving and valley filling under the normal weather condition. Under severe and extreme weather conditions, the ESS can also ensure the continuous power supply for loads as much as possible. Overall, the ESS can improve the economy and security of ADNs under normal, severe, and extreme weather conditions. This paper exploits the potential of the ESS in terms of safety support, and balances its safety and economy to provide emergency power supply for loads. The modified IEEE 33-node test system is employed to verify the feasibility of the proposed method.

This paper proposes a new idea for ESS planning that can be applied to ADNs where disastrous weather occurs frequently to enhance the resilience. However, due to the limited scale of ESS, other flexible resources of ADNs, such as microgrids and flexible loads, can be considered in the future research.

Appendix A

TABLE AI
Failure Rates of Distribution Lines Under Different Weather Conditions

Line			Failure rate (occurrence/day)		
Number	From	To	Normal	Severe	Extreme
1	1	2	0.0024	0.0327	0.2383
2	2	3	0.0131	0.1748	0.6395
3	2	19	0.0097	0.1297	0.5490
4	3	4	0.0101	0.1351	0.5717
5	3	23	0.0217	0.1903	0.3285
6	4	5	0.0050	0.0664	0.2808
7	5	6	0.0189	0.2522	0.2671
8	6	7	0.0273	0.2651	0.5450
9	6	26	0.0277	0.1701	0.5660
10	7	8	0.0052	0.0697	0.2949
11	8	9	0.0099	0.1327	0.5616
12	9	10	0.0389	0.5204	0.3020
13	10	11	0.0144	0.1920	0.3124
14	11	12	0.0157	0.2095	0.3865
15	12	13	0.0198	0.2646	0.3195
16	13	14	0.0342	0.2570	0.4335
17	14	15	0.0194	0.2595	0.2980
18	15	16	0.0043	0.0581	0.2460
19	16	17	0.0399	0.2332	0.2563
20	17	18	0.0109	0.1452	0.6143
21	19	20	0.0188	0.2513	0.4634
22	20	21	0.0120	0.1600	0.6768
23	21	22	0.0238	0.3183	0.3470
24	23	24	0.0237	0.3176	0.3440
25	24	25	0.0054	0.0720	0.3045
26	26	27	0.0075	0.1007	0.4263
27	27	28	0.0281	0.2754	0.5885
28	28	29	0.0213	0.2851	0.2063
29	29	30	0.0134	0.1799	0.3613
30	30	31	0.0258	0.2454	0.4616
31	31	32	0.0082	0.1101	0.4658
32	32	33	0.0090	0.1209	0.5115
33	21	8	0.0330	0.2090	0.4400
34	9	15	0.0330	0.2090	0.4400
35	12	22	0.0330	0.2090	0.4400
36	18	33	0.0133	0.1773	0.3500
37	25	29	0.0133	0.1773	0.3500

References

[1] E. Ciapessoni, D. Cirio, A. Pitto *et al.*, "A quantitative methodology to assess the process of service and infrastructure recovery in power systems," *Electric Power Systems Research*, vol. 189, pp. 1-8, Aug.

2020.
[2] U.S. Energy Information Administration. (2017, Sept.). U.S. Energy Information Administration report. [Online]. Available: https://www. eia. gov/todayinenergy/detail.php?id=32992
[3] Bill Magness. (2021, Mar.). Review of February 2021 extreme cold weather event – ERCOT presentation. [Online]. Available: http://www. ercot.com/content/wcm/key_documents_lists/225373/2.2_REVISED_ERCOT_Presentation.pdf
[4] M. S. Khomami, M. T. Kenari, and M. S. Sepasian, "A warning indicator for distribution network to extreme weather events," *International Transactions on Electrical Energy Systems*, vol. 29, no. 8, pp. 1-15, Mar. 2019.
[5] R. E. Brown, "Hurricane hardening efforts in Florida," in *Proceedings of* 2008 *IEEE PES General Meeting – Conversion and Delivery of Electrical Energy in the 21st Century*, Pittsburgh, USA, Jul. 2008, pp. 1-7.
[6] S. Mousavizadeh, A. Alahyari, S. R. M. Ghodsinya *et al*., "Incorporating microgrids coupling with utilization of flexible switching to enhance self-healing ability of electric distribution systems," *Protection and Control of Modern Power Systems*, vol. 6, pp. 1-11, Jul. 2021.
[7] M. Panteli and D. S. Kirschen, "Situation awareness in power systems: theory, challenges and applications," *Electric Power Systems Research*, vol. 122, pp. 140-151, May 2015.
[8] Z. Bie, C. Lin, and G. Li. "Development and prospect of resilient power system in the context of energy transition," *Proceedings of the CSEE*, vol. 40 no. 9, pp. 2735-2745, May 2020.
[9] S. Khazeiynasab and J. Qi, "Resilience analysis and cascading failure modeling of power systems under extreme temperatures," *Journal of Modern Power Systems and Clean Energy*, vol. 9, no. 6, pp. 1446-1457, Nov. 2021.
[10] M. Naguib, W. A. Omran, and H. E. A. Talaat, "Performance enhancement of distribution systems via distribution network reconfiguration and distributed generator allocation considering uncertain environment," *Journal of Modern Power Systems and Clean Energy*, vol. 10, no. 3, pp. 647-655, May 2022.
[11] G. Zhang, F. Zhang, X. Zhang *et al.*, "Mobile emergency generator planning in resilient distribution systems: a three-stage stochastic model with nonanticipativity constraints," *IEEE Transactions on Smart Grid*, vol. 11, no. 6, pp. 4847-4859, Nov. 2020.
[12] S. Ma, L. Su, Z. Wang *et al.*, "Resilience enhancement of distribution grids against extreme weather events," *IEEE Transactions on Power Systems*, vol. 33, no. 5, pp. 4842-4853, Sept. 2018.
[13] S. Ma, B. Chen, and Z. Wang, "Resilience enhancement strategy for distribution systems under extreme weather events," *IEEE Transactions on Smart Grid*, vol. 9, no. 2, pp. 1442-1451, Mar. 2018.
[14] W. Yuan, J. Wang, F. Qiu *et al.*, "Robust optimization-based resilient distribution network planning against natural disasters," *IEEE Transactions on Smart Grid*, vol. 7, no. 6, pp. 2817-2826, Nov. 2016.
[15] M. Nazemi, M. Moeini-Aghtaie, M. Fotuhi-Firuzabad *et al.*, "Energy storage planning for enhanced resilience of power distribution networks against earthquakes," *IEEE Transactions on Sustainable Energy*, vol. 11, no. 2, pp. 795-806, Apr. 2020.
[16] Q. Zhang, Z. Wang, S. Ma *et al.*, "Stochastic pre-event preparation for enhancing resilience of distribution systems," *Renewable & Sustainable Energy Reviews*, vol. 152, p. 111636, Dec. 2021.
[17] X. Wu and A. J. Conejo, "An efficient tri-level optimization model for electric grid defense planning," *IEEE Transactions on Power Systems*, vol. 32, no. 4, pp. 2984-2994, Jul. 2017.
[18] H. Zhang, S. Ma, T. Ding *et al.*, "Multi-stage multi-zone defender-attacker-defender model for optimal resilience strategy with distribution line hardening and energy storage system deployment," *IEEE Transactions on Smart Grid*, vol. 12, no. 2, pp. 1194-1205, Mar. 2021.
[19] Y. Liu, L. Guo, C. Wang *et al.*, "Economic dispatch of microgrid based on two stage robust optimization," *Proceedings of the CSEE*, vol. 38, no. 14, pp. 4013-4022, Jul. 2018.
[20] R. T. Rockafellar and R. J.-B. Wets, "Scenarios and policy aggregation in optimization under uncertainty," *Mathematics of Operations Research*, vol. 16, no. 1, pp. 119-147, Feb. 1991.
[21] J. Wang, X. Xiong, Z. Li *et al*., "Time distribution of weather-related transmission line failure and its fitting," *Electric Power Automation Equipment*, vol. 36, no. 3, pp. 109-114, Mar. 2016.
[22] H. Chen, T. Cong, W. Yang *et al.*, "Progress in electrical energy storage system: a critical review," *Progress in Natural Science*, vol. 19, no. 3, pp. 291-312, Mar. 2009.
[23] B. Dunn, H. Kamath, and J. M. Tarascon, "Electrical energy storage for the grid: a battery of choices," *Science*, vol. 334, no. 6058, pp. 928-935, Nov. 2011.
[24] X. Li, R. Ma, W. Gan *et al.*, "Optimal dispatch for battery energy storage station in distribution network considering voltage distribution improvement and peak load shifting," *Journal of Modern Power Systems and Clean Energy*, vol. 10, no. 1, pp. 131-139, Jan. 2022.
[25] J. Li, Y. Xue, L. Tian *et al*., "Research on optimal configuration strategy of energy storage capacity in grid-connected microgrid," *Protection and Control of Modern Power Systems*, vol. 2, no. 4, pp. 389-396, Dec. 2017.
[26] M. Panteli and P. Mancarella, "The grid: stronger, bigger, smarter?: Presenting a conceptual framework of power system resilience," *IEEE Power and Energy Magazine*, vol. 13, no. 3, pp. 58-66, Apr. 2015.
[27] X. Chen, W. Wu, and B. Zhang, "Robust restoration method for active distribution networks," *IEEE Transactions on Power Systems*, vol. 31, no. 5, pp. 4005-4015, Sept. 2016.
[28] S. Lei, C. Chen, Y. Song *et al*., "Radiality constraints for resilient reconfiguration of distribution systems: formulation and application to microgrid formation," *IEEE Transactions on Smart Grid*, vol. 11, no. 5, pp. 3944-3956, Sept. 2020.
[29] W. Wang, X. Xiong, Y. He *et al*., "Scheduling of separable mobile energy storage systems with mobile generators and fuel tankers to boost distribution system resilience," *IEEE Transactions on Smart Grid*, vol. 13, no. 1, pp. 443-457, Jan. 2022.
[30] X. Xiong, J. Wang, J. Yuan *et al*., "Temporal and spatial environments dependent power grid failure method and its application in power grid reliability assessment," *Power System Protection and Control*, vol. 43, no. 15, pp. 28-35, Aug. 2015.
[31] Q. Shi, F. Li, T. Kuruganti *et al*., "Resilience-oriented dg siting and sizing considering stochastic scenario reduction," *IEEE Transactions on Power Systems*, vol. 36, no. 4, pp. 3715-3727, Jul. 2021.
[32] Y. Fan and C. Liu, "Solving stochastic transportation network protection problems using the progressive hedging-based method," *Networks and Spatial Economics*, vol. 10, no. 2, pp. 193-208, Mar. 2008.
[33] J. P. Watson and D. L. Woodruff, "Progressive hedging innovations for a class of stochastic mixed-integer resource allocation problems," *Computational Management Science*, vol. 8, no. 4, pp. 355-370, Jul. 2010.
[34] L. Shang, B. Wei, W. Wang *et al*., "A planning method of dynamic energy storage configuration in an active distribution network," *Power System Protection and Control*, vol. 48, No. 17, pp. 84-92, Sept. 2020.
[35] J. Wang, J. Yao, Z. Liu *et al*., "Fault statistical analysis and probability distribution fitting for a power distribution network in adverse weather conditions," *Power System Protection and Control*, vol. 50, no. 17, pp. 143-153, Sept. 2022.
[36] M. Panteli, C. Pickering, S. Wilkinson *et al.*, "Power system resilience to extreme weather: fragility modeling, probabilistic impact assessment, and adaptation measures," *IEEE Transactions on Power Systems*, vol. 32, no. 5, pp. 3747-3757, Sept. 2017.

Hongzhou Chen received the B. E. degree in electrical engineering from China University of Petroleum (East China), Qingdao, China. He is currently pursuing the Ph. D. degree with the School of Electrical Engineering, Chongqing University, Chongqing, China. His research interests include power system resilience, resources allocation, and electricity market.

Jian Wang received the B. E. and Ph. D. degrees in electrical engineering from Chongqing University, Chongqing, China, in 2010 and 2016, respectively, where he is currently an Associate Professor with the School of Electrical Engineering, Chongqing University. He was a Postdoctoral Fellow with the Department of Electrical and Computer Engineering, University of Alberta, Edmonton, Canada, from October 2018 to September 2019. His research interests include power system protection and control, risk early warning of meteorological disaster for power grids.

Jizhong Zhu received the B.S., M.S., and Ph.D. degrees in electrical engineering from Chongqing University, Chongqing, China, in 1985, 1987, and 1990, respectively. His work experience includes Chongqing University, Brunel University, London, UK, National University of Singapore, Singapore, Howard University, Washington, USA, Alstom Grid, Redmond, USA, and Electric Power Research Institute of China Southern Power Grid, Guangzhou, China. He is a Fellow of IEEE and a Professor at School of Electric Power, South China University of Technology, Guangzhou, China. His research interests include power system operation and control as well as renewable energy application.

Xiaofu Xiong received the B.E., M.E., and Ph.D. degrees in electrical engi-

neering from Chongqing University, Chongqing, China, in 1982, 1986, and 2005, respectively, where he is currently a Professor with the School of Electrical Engineering. His current research interests include power system protection and control, power system resilience, and risk analysis.

Wei Wang received the B. E. degree in electrical engineering from Southwest Jiaotong University, Chengdu, China, in 2014, and the M.E. and the Ph. D. degrees in electrical engineering from Chongqing University, Chongqing, China, in 2017 and 2021, respectively. He is currently a Postdoctoral Researcher with the Electric Power Research Institute, State Grid Chongqing Electric Power Company, Chongqing, China. His research interests include power system resilience, mathematical programming, energy management of microgrids, and power system protection and control.

Hongrui Yang received the B. E. degree in electrical engineering from Chongqing University, Chongqing, China. He is currently pursuing the Ph.D. degree with the School of Electrical Engineering, Chongqing University. His research interests include smart grid and fractional frequency transmission system.